Particuology 18 (2015) 89–95

Contents lists available at ScienceDirect

Particuology

journal homepage: www.elsevier.com/locate/partic

Light attenuation cross-section of black carbon in an urban atmosphere in northern China☆

Junji Cao[a,b,*], Chongshu Zhu[a], Kinfai Ho[c], Yongming Han[a], Zhenxing Shen[d], Changlin Zhan[e], Jiaquan Zhang[e]

[a] Key Laboratory of Aerosol Chemistry and Physics, State Key Laboratory of Loess and Quaternary Geology, Institute of Earth Environment, Chinese Academy of Sciences, Xi'an 710075, China
[b] Institute of Global Environmental Change, Xi'an Jiaotong University, Xi'an 710049, China
[c] The Jockey Club School of Public Health and Primary Care, The Chinese University of Hong Kong, Shatin, Hong Kong, China
[d] Department of Environmental Science and Engineering, Xi'an Jiaotong University, Xi'an 710049, China
[e] School of Environmental Science and Engineering, Hubei Polytechnic University, Hubei Key Laboratory of Mine Environmental Pollution Control and Remediation, Huangshi 435000, China

ARTICLE INFO

Article history:
Received 2 September 2013
Received in revised form 28 March 2014
Accepted 2 April 2014

Keywords:
Light attenuation cross-section
Elemental carbon
Dust
Xi'an

ABSTRACT

Fine particulate matter ($PM_{2.5}$) samples were collected over two years in Xi'an, China to investigate the relationships between the aerosol composition and the light absorption efficiency of black carbon (BC). Real-time light attenuation of BC at 880 nm was measured with an aethalometer. The mass concentrations and elemental carbon (EC) contents of $PM_{2.5}$ were obtained, and light attenuation cross-sections (σ_{ATN}) of $PM_{2.5}$ BC were derived. The mass of EC contributed ~5% to $PM_{2.5}$ on average. BC σ_{ATN} exhibited pronounced seasonal variability with values averaging 18.6, 24.2, 16.4, and 26.0 m^2/g for the spring, summer, autumn, and winter, respectively, while averaging 23.0 m^2/g overall. σ_{ATN} varied inversely with the ratios of EC/$PM_{2.5}$, EC/[SO_4^{2-}], and EC/[NO_3^-]. This study of the variability in σ_{ATN} illustrates the complexity of the interactions among the aerosol constituents in northern China and documents certain effects of the high EC, dust, sulfate and nitrate loadings on light attenuation.

Introduction

Aerosol species, including carbonaceous matter, dust, sulfate, and nitrate, are critically important to the radiative balance of the atmosphere (Crutzen & Andreae, 1990). Aerosols are major light absorbers in atmosphere due to their contents of light-absorbing substances, such as elemental carbon (EC) and hematite (α-Fe_2O_3). The absorption of solar radiation can lead to a warming effect similar to that caused by greenhouse gases, thereby possibly affecting the atmospheric stability over regional scales; these changes could alter the hydrological cycle and possibly cause other effects (Jacobson, 2001; Ramanathan et al., 2005).

The specific attenuation cross-section (σ_{ATN}) of BC is a critical parameter for light absorption calculations. This coefficient depends on the size distribution and fractal dimensions of BC, as well as its mixing state relative to other components. BC can exist in two mixing states: externally mixed with other particles or internally incorporated within other particles or as a core surrounded by a well-mixed shell (Haywood, Roberts, Slingo, Edwards, & Shine, 1997; Jacobson, 2000, 2001; Myhre, Stordal, Restad, & Isaksen, 1998). Obtaining accurate values for σ_{ATN} is currently challenging due to the effects of the mixing state and other factors (Arnott, Hamasha, Moosmüller, Sheridan, & Ogren, 2005; Weingartner et al., 2003). The literature values for σ_{ATN} vary over an order of magnitude, ranging from 5 to 55 m^2/g (Jeong, Hopke, Kim, & Lee, 2004; Liousse, Cachier, & Jennings, 1993). Because roughly one-fourth of the global BC emissions are believed to originate from China (Cooke, Liousse, Cachier, & Feichter, 1999), the high loading of BC in the

☆ This paper is adapted from the presentation at the 11th National Aerosol Conference and 10th Cross-Strait Workshop for Aerosol Science and Technology, May 16–19, Wuhan, China, as recommended by Prof. Junji Cao, the chair of the scientific committee.

* Corresponding author at: Key Laboratory of Aerosol Chemistry and Physics, State Key Laboratory of Loess and Quaternary Geology, Institute of Earth Environment, Chinese Academy of Sciences, Xi'an 710075, China. Tel.: +86 29 88326488; fax: +86 2988320456.
E-mail addresses: cao@loess.llqg.ac.cn, jjcao@ieecas.cn (J. Cao).

http://dx.doi.org/10.1016/j.partic.2014.04.011
1674-2001/

atmosphere over China and its effect on the balance of solar radiation have serious implications for regional climatic change (Menon, Hansen, Nazarenko, & Luo, 2002).

Northern China often suffers from high loadings of air pollutants, particularly EC, dust, sulfate, and nitrate (Cao et al., 2007, 2009, 2012; Zhang et al., 2011); the interactions among these substances can alter their interactions with light, including the positive forcing from BC. However, no published data describing BC σ_{ATN} are available for $PM_{2.5}$ in China. Therefore, the purpose of this study is to characterize the σ_{ATN} at Xi'an, which is a large city in northwestern China and to investigate the relationships between various aerosol species. These results will help to evaluate σ_{ATN} and to understand the effects of urban aerosols on light attenuation in other regions of China.

Methods

Xi'an (34.2° N, 108.9° E), which is in Shaanxi Province, is the largest city in northwestern China and has a population of eight million. Xi'an also experiences the air pollution typical of many Chinese cities; high dust loadings (it is near Asian dust source regions) are often present with low relative humidity (RH). Elevated carbonaceous aerosol loadings contribute to the high PM levels (Cao, Wu, et al., 2005).

Samples of $PM_{2.5}$ were collected in Xi'an from 13 September 2003 to 31 August 2005 on the rooftop of a building ~10 m above ground at Institute of Earth Environment, Chinese Academy of Sciences, Xi'an. $PM_{2.5}$ samples were collected daily using MiniVol $PM_{2.5}$ Portable Air Sampler (Airmetrics Inc., 2095 Garden Ave. Suite 102 Eugene, OR 97403, U.S.A.) operating at 5 L/min (Cao et al., 2003; Cao, Wu, et al., 2005). The mass concentrations of $PM_{2.5}$ were determined gravimetrically using a Sartorius MC5 electronic microbalance (Sartorius, Gottingen, Germany) with a ±1 μg sensitivity. The EC contents were measured with a DRI-2001 carbon analyzer operated according to the IMPROVE thermal/optical reflectance (IMPROVE/TOR) protocol (Chow & Watson, 2002). The instrumental detection limit for the EC was 0.19 μg; this amount is equal to a mass concentration of 0.37 μg/m^3 under the experimental conditions used in this work. The quality assurance/quality control (QA/QC) procedures have been described in Cao et al. (2003).

The light attenuation was recorded at 5-min intervals using an aethalometer (Model AE-16, Magee Scientific) with a $PM_{2.5}$ inlet and a flow rate of 4 L/min. This instrument collects particles on a quartz fiber tape and measures the light attenuation caused by the sampled particles. The attenuation (ATN, in Mm^{-1}), which is measured at 880 nm, was determined based on the following equation:

$$\mathrm{ATN} = 100 \ln\left(\frac{I}{I_0}\right). \quad (1)$$

In this equation, I and I_0 are the transmitted light intensities for the loaded filter and the blank, respectively. The factor of 100 is used for numerical convenience. The measured light attenuation can be converted into BC concentrations [BC], as follows:

$$[\mathrm{BC}] = \frac{\mathrm{ATN}}{\sigma_{ATN}}, \quad (2)$$

where σ_{ATN} is the specific attenuation cross-section of the particle-laden filter (m^2/g). We note that the light-attenuation measurements made through the filters used by the aethalometers can be influenced by several factors unrelated to BC mass (Weingartner et al., 2003). In this work, the manufacturer's default value (16.6 m^2/g) for σ_{ATN} was used to calculate the BC concentrations. In addition, 206,600 individual 5-min BC concentrations were used to calculate the daily averages of the total BC. Due to instrument failures, the data were missing from May to June 2004 and for several other shorter periods (one or two days) (Table 1). In this instance, the EC was obtained by using the IMPROVE/TOR protocol, while BC refers to what was measured by the aethalometer. Previous studies have reported the differences between EC and BC (Andrea & Gelencsér, 2006).

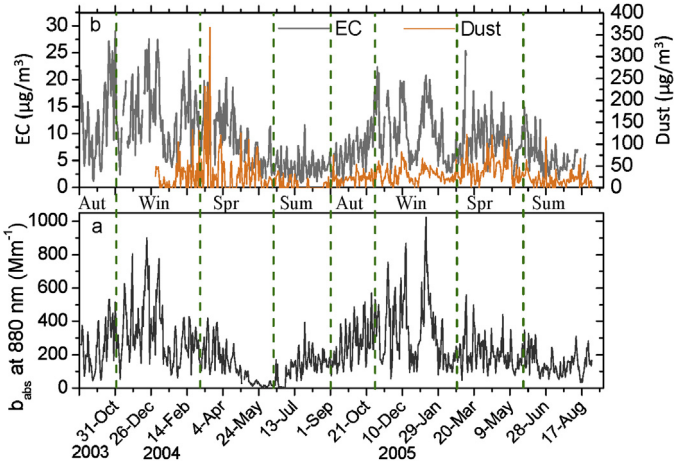

Fig. 1. Time series for (a) aerosol light absorption coefficient (b_{abs}) at 880 nm, and (b) concentrations of dust and EC.

The mineral dust loadings were estimated from the Fe concentrations, which were determined through a proton-induced X-ray emission (PIXE) technique while assuming that the Fe constituted 4% of mineral dust content (Zhang et al., 2003). The PIXE analyses were performed using the 2.5 MeV protons with a 50 nA beam current, which was produced by 2 × 1.7 MV tandem accelerator at Beijing Normal University (GIC4117, General Ionex Corp.). The PIXE trace element data were corrected for the background by using blank filters, specifically, filters brought to the field and installed in the samplers but through which no air was pumped.

A Dionex-600 Ion Chromatograph (Dionex Inc., Sunnyvale, CA, USA) was used to determine the contents of both the cations and the anions in the aqueous extracts of the air filters. The instrument was equipped with an IonPacCS12A column (20 mM methanesulfonic acid as the eluent) to analyze the cations, while an IonPac AS14A column (8 mM Na_2CO_3/1 mM $NaHCO_3$ as the eluent) was used to analyze the anions. The minimum detection limits were as follows: 0.001 μg/mL for Na^+, NH_4^+, K^+, Mg^{2+}, and Ca^{2+}; 0.008 μg/mL for Cl^-, 0.025 μg/mL for NO_3^-; 0.027 μg/mL for SO_4^{2-}. Standard reference materials produced by the National Research Center for Certified Reference Materials (Beijing, China) were analyzed for quality control and quality assurance purposes. All of the reported ion concentrations were corrected using the field blanks. The experimental uncertainties were ±0.04 for NO_3^- and SO_4^{2-}, ±0.03 for Ca^{2+}, ±0.02 for Cl^-, ±0.01 for NH_4^+, K^+ and Mg^{2+}, and ±0.004 for Na^+.

Results and discussion

Aerosol light absorption

The aerosol light absorption coefficient (b_{abs}) at 880 nm showed relatively low values in summer and high values in winter that ranged from 15.0 to 1025.0 Mm^{-1} and averaged 241 Mm^{-1} over the entire sampling period (Fig. 1(a)). The seasonally averaged values were 184.0, 142.8, 248.0, 329.0 Mm^{-1} for the spring (March, April, and May), summer (June, July, and August), autumn (September and October) and winter (November, December, January, and February), respectively. The present results were higher than the

Table 1
Monthly and annual averages and standard deviations of the aerosol measurements.

2003–2005	Number of samples	BC (μg/m^3)	EC (μg/m^3)	$PM_{2.5}$ (μg/m^3)	Dust (μg/m^3)	EC/$PM_{2.5}$
January	62	22.2 ± 12.8	12.1 ± 5.7	294.6 ± 145.2	25.0	0.04
February	57	13.5 ± 5.9	9.4 ± 4.6	199.5 ± 71.2	25.6	0.05
March	59	14.3 ± 6.8	10.5 ± 4.1	194.8 ± 86.7	44.4	0.05
April	56	10.8 ± 4.1	10.1 ± 3.3	150.6 ± 48.3	40.8	0.07
May	29	10.3 ± 4.2	8.1 ± 2.8	163.2 ± 67.7	37.8	0.05
June	27	9.9 ± 4.7	5.9 ± 3.0	109.4 ± 48.3	18.0	0.05
July	55	7.9 ± 3.9	4.2 ± 2.0	101.7 ± 41.4	9.9	0.04
August	55	9.9 ± 3.6	4.6 ± 1.7	129.6 ± 44.3	12.1	0.04
September	47	12.0 ± 5.9	6.5 ± 3.5	116.3 ± 52.3	18.2	0.06
October	60	17.3 ± 8.0	11.0 ± 5.9	166.3 ± 82.1	24.2	0.07
November	55	20.8 ± 10.6	12.4 ± 5.2	238.0 ± 125.8	28.5	0.05
December	54	23.5 ± 12.6	12.7 ± 5.4	290.3 ± 143.3	32.1	0.04
Annual	616	14.9 ± 9.4	9.2 ± 5.2	185.4 ± 110.6	26.5	0.05

BC concentrations were estimated using $\sigma_{ATN} = 16.6\ m^2/g$; dust concentrations were estimated using Fe/0.04.

values observed while studying the PM_{10} in some urban and rural areas of China (Zhang et al., 2008). This high absorption at Xi'an degrades visibility and causes other atmospheric and environmental effects. The data for the EC concentrations (Fig. 1(b)) vary similarly to those for aerosol light absorption (Fig. 1(a)). The strong correlation between the daily averaged aerosol light absorption and EC loadings implies that the aerosol light absorption was mainly caused by EC. In addition, the EC presented a similar degree of

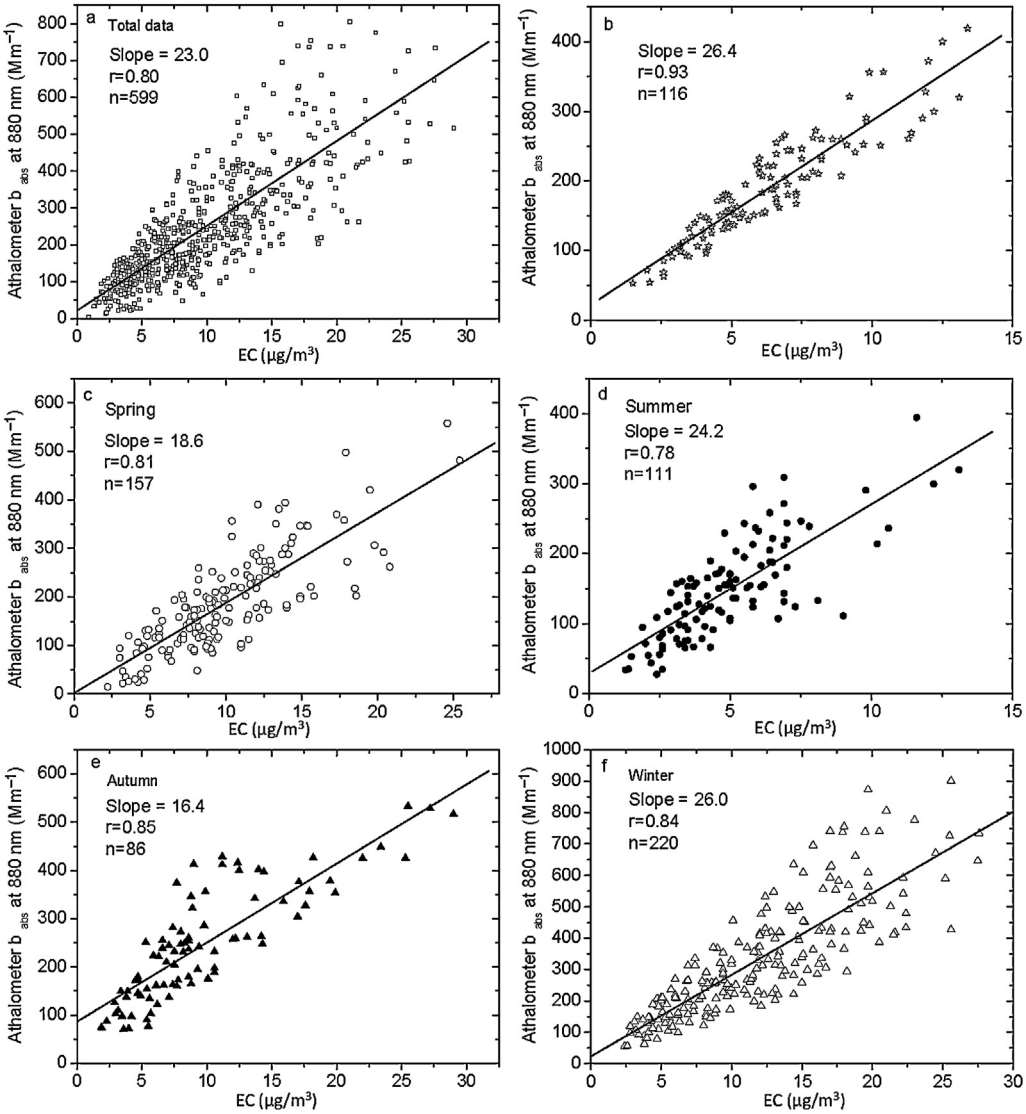

Fig. 2. Correlations between the daily averaged aerosol light absorptions at 880 nm and the 24-h EC concentrations for all of the samples: (a) total data, (b) samples with little or no dust loading, (c) spring, (d) summer, (e) autumn, and (f) winter.

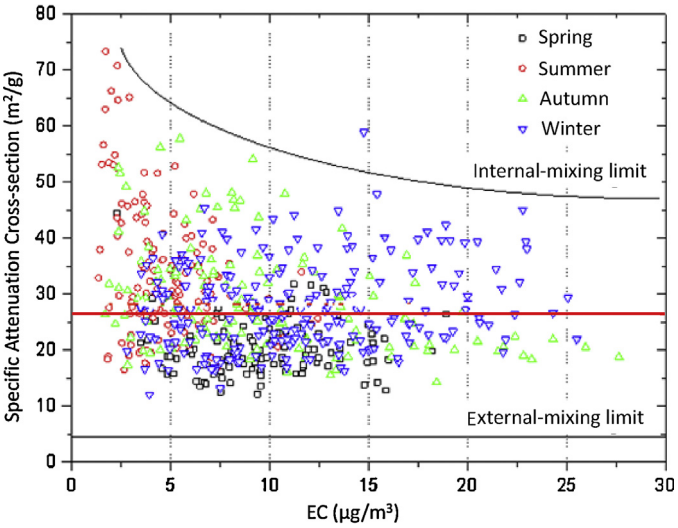

Fig. 3. Variations in σ_{ATN} along the EC level. The red solid line represents the annual average level. (For interpretation of the references to color in this figure legend, the reader is referred to the web version of the article.)

variability compared to light absorption; the values ranged from 1.3 to 29.0 μg/m^3, averaging 9.6 μg/m^3. Across the seasons, high EC concentrations were observed during the winter, averaging ~11.6 μg/m^3, while relatively lower values were observed during the summer (~5.0 μg/m^3).

The dust concentrations were estimated from the Fe data, and relatively low dust loadings were observed in summer, averaging 13.0 μg/m^3. However, some high dust loadings were found in spring, which averaged 41.0 μg/m^3; These high loadings were attributed to local and transported dust, as well as construction activities. Table 1 summarizes the monthly averages of the aerosol measurements from September 2003 to August 2005. In general, the ambient concentrations of BC and EC varied synchronously with that of $PM_{2.5}$. The ratio of EC to $PM_{2.5}$ remained relatively stable, ranging from 0.04 to 0.07 and averaging 0.05. The high BC and EC concentrations in December were approximately 2–3 times the low values in July. This phenomenon can be explained by the buildup of air pollutants in winter; therefore, the aerosol was dominated by local emission sources and was also affected by meteorological conditions (Cao, Wu, et al., 2005).

Relationship between the aerosol light absorption and EC

Fig. 2 shows the robust linear correlation between the $PM_{2.5}$ light absorption at 880 nm and the EC. Strong correlations (r: 0.78–0.85) were found for parallel 24-h sample data across the four seasons, suggesting that the overall absorption was dominated by EC at Xi'an. A linear regression between the Aethalometer™ b_{abs} values and EC concentrations for the entire data generates an average slope of σ_{ATN} = 23.0 m^2/g at 880 nm. The seasonal averages for the σ_{ATN} values calculated using this method were 18.6, 24.2, 16.4, and 26.0 m^2/g in the spring, summer, autumn, and winter, respectively. High correlation coefficients (r = 0.93) were obtained during periods with little or no dust loading; the slope of linear regression corresponds to a value of σ_{ATN} = 26.4 m^2/g. This strong relationship implies that the main contributors to the aerosol light absorption were EC particles. The different values of the σ_{ATN} over the four seasons are attributed to changes in the relative proportions of EC and dust in the aerosol particles and other influencing factors.

Seasonal variations of σ_{ATN}

Fig. 3 illustrates the diversity in σ_{ATN} as a function of the EC loadings. For cases where EC < 5 μg/m^3, the values of σ_{ATN} varied by a factor of six, ranging from 12.0 to 73.3 m^2/g. As the EC concentrations increased, the values of σ_{ATN} converged toward an average value (~26 m^2/g). This phenomenon agrees with the trend observed for the Taibei urban atmosphere (Chou et al., 2005); however, the reasons for this variability in σ_{ATN} remain unclear. The optical properties of graphite set a fixed lower limit for the σ_{ATN} of the externally mixed aerosol constituents (Petzold, Kopp, & Niessner, 1997). This boundary is also known as the "external-mixing limit," and a value of 4 m^2/g is used in this study. In addition, the data are also limited by a concave upper boundary. Previous investigators have shown that the σ_{ATN} of internally mixed aerosols depends on the physico-chemical properties of the EC particles, specifically their size distribution, morphology, mixing state, etc. (Petzold et al., 1997). Therefore, the "internal-mixing limit" shown in Fig. 3 is a conceptual reference. More importantly, all of the σ_{ATN} values in our study were higher than 4 m^2/g, indicating that the EC particles in the Xi'an atmosphere were internally mixed with transparent aerosol species.

The frequency distributions for σ_{ATN} varied between the four seasons; these data and the seasonally averaged values for EC, BC, and $PM_{2.5}$ mass are plotted in Fig. 4. The median σ_{ATN} values attained a maximum (33.7 m^2/g) during the summer and a minimum (20.0 m^2/g) during the spring; therefore, the highest maximum to minimum ratio for the seasonally averaged data was 1.7. This seasonal variability differs from what was observed at the Jungfraujoch high-alpine research station in Switzerland. At that location, the seasonal variations (σ_{ATN} = 8.9, 9.5, 10.9, and 9.9, for spring, summer, autumn and winter, respectively) (Lavanchy, Gaggeler, Nyeki, & Baltensperger, 1999) were much smaller than what was observed at Xi'an. The relatively weak seasonality in the σ_{ATN} at the Jungfraujoch was explained by physical transformations of the carbonaceous particles in the aged air sampled at that remote site.

Several extremely high values for σ_{ATN} were found during the summer in our study (Fig. 4), and these values can be ascribed to the dominance of internally mixed particles (Fig. 3). Indeed, the formation of secondary sulfate- and nitrate-rich particles is favored by the warm and relatively moist conditions encountered during the summer and autumn. The high σ_{ATN} values observed during the summer and autumn can be attributed to the biomass burned during the harvest season. These effects occur because Xi'an is situated in the Guanzhong Plain, which is a base for food production in China. In this regard, Novakov and Corrigan (1995) reported that potassium, which was elevated in emissions attributed to burning biomass, exerted a catalytic effect on EC, lowering its volatilization temperature and possibly causing negative EC artifacts. These phenomena could contribute to the high σ_{ATN} values observed.

A previous study (Liousse et al., 1993) revealed that σ_{ATN} is affected by both aerosol sources and by particle aging during transport. The surface coatings may include various organic, ionic, or mineral substances that might affect refractive indices of particles and contribute to the variability in the σ_{ATN}. The thickness of the coatings affects the mass absorption efficiency more than the type of coating because the refractive indices for organic compounds and inorganic salts are relatively similar (Bergstrom, 1982; Rosen & Hansen, 1984). Rearranging Eq. (2) reveals that $b_{abs} = \sigma_{ATN}$[BC]. Therefore, increasing the light absorption should increase σ_{ATN}. The highest seasonal median value for σ_{ATN} occurred in summer due to several factors: (i) the influences of several anomalously high values attributed to biomass burning, (ii) a relatively large increase in the symmetrical particles and cluster-like structures emitted from

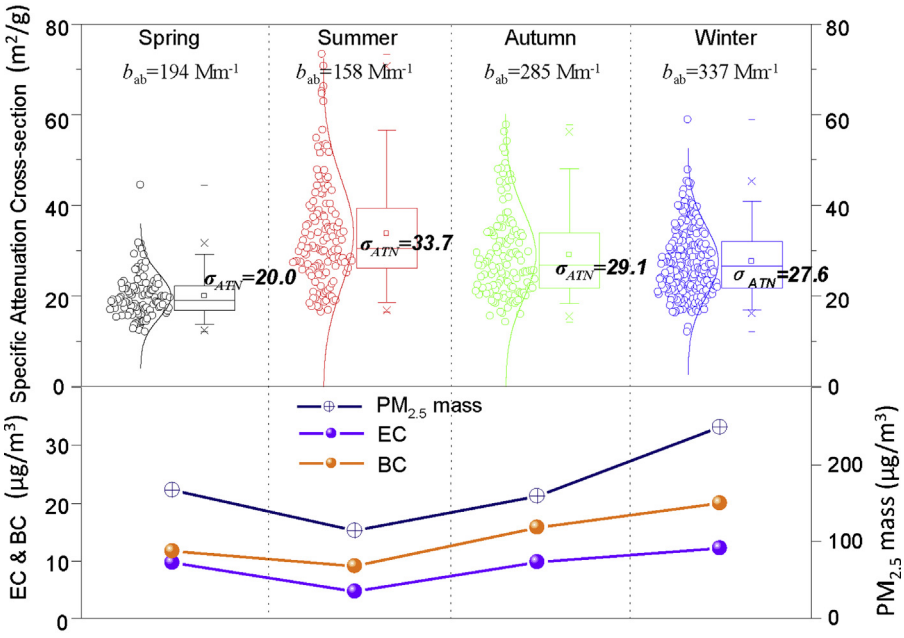

Fig. 4. Seasonal variations in the σ_{ATN}, the concentrations of EC, BC and $PM_{2.5}$ mass. The box plots in upper portion of the figure indicate the mean 24-h concentration and the min, 1st, 25th, 50th, 75th, 99th, and max percentiles. A normal curve is fitted to the measurements. The EC, BC, and $PM_{2.5}$ mass were averaged seasonally and plotted in the lower portion of the figure.

the motor vehicles, and (iii) the enhancement of the secondary and aged aerosols under high RH (60–80%) and strong solar radiation.

In related studies, Jeong et al. (2004) concluded that the σ_{ATN} values measured in Philadelphia, USA might have increased due to the hygroscopic nature of carbonaceous materials during sulfate-haze events. Martins et al. (1998) reported that samples containing asymmetrical particles and cluster-like structures exhibited high σ_{ATN} values, while samples with low σ_{ATN} values contained mostly homogeneous particles. As noted above, changes in light absorption properties and volatilization artifacts during the thermal measurements also can arise from internal mixing. The highest average BC and EC loadings in our study occurred during the winter (Fig. 4) and the proportions of fly ash particles increased at that time of year because large quantities of coal were burned to heat residences (Cao, Wu, et al., 2005). These particles were often spheroidal in shape, and they may contribute to the lower σ_{ATN} values in winter compared to the values observed during the summer and autumn.

Interestingly, the lowest median seasonal value for σ_{ATN} occurred in the spring (20.0 m^2/g in Fig. 4). Xi'an is located in the Loess Plateau and, during the spring, this region is often affected by high loadings of mineral dust transported from upwind arid and semi-arid regions, as well as re-suspended and local fugitive dust (Cao, Lee, et al., 2005). Previous studies have demonstrated that Asian dust particles cause light absorption in the Asian-Pacific region (Clarke & Charlson, 1985; Hansen, Kapustin, Kopeikin, Gillette, & Bodhaine, 1993; Li et al., 2006) due to hematite, which is a natural component of dust.

Hematite is the only commonly occurring substance with a light absorption coefficient comparable to EC in the near ultraviolet range (Bohren & Huffman, 1983), but its absorption rapidly decreases in the visible light range. Because mineral dust has low absorption efficiency (ranging from 0.02 to 0.1 m^2/g at 550 nm, Clarke & Charlson, 1985), the mineral dust loading would need to exceed that of BC by at least two orders-of-magnitude to exert a significant influence on σ_{ATN} (Hansen et al., 1993). These high loadings are occasionally exceeded during heavy Asian dust storms (Cao, Lee, et al., 2005), but no such storms occurred during our observation period. Therefore, the influence of the mineral dust should be negligible (less than 0.1–1% of σ_{ATN}) under conditions without dust storms. This conclusion counters the results of Li et al. (2006), who concluded that the contributions of mineral dust to light absorption reached 19–31% during the autumn and winter, respectively, in Xi'an. This discrepancy may be explained by their use of uncorrected σ_{ATN} values for mineral dust (2.7 m^2/g in autumn, 4.4 m^2/g in winter).

We can relate the BC mass concentrations (μg/m^3) to σ_{ATN} to derive the absorption coefficients (b_{abs}, Mm^{-1}). The average b_{abs} values for the four seasons were 194, 158, 285, and 337 Mm^{-1} for the spring, summer, autumn, and winter, respectively, as shown in Fig. 4. Mader, Flagan, and Seinfeld (2002) found that the average

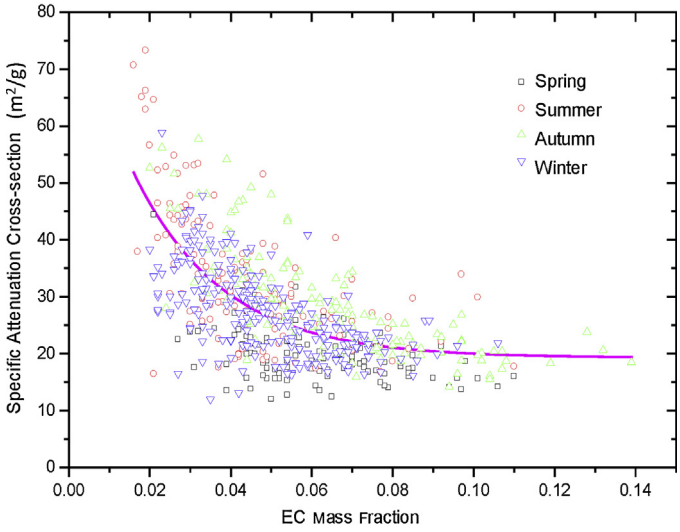

Fig. 5. Relationship between the σ_{ATN} and the EC mass fraction in the particulate matter (EC/$PM_{2.5}$). The magenta solid curve is a negative exponential curve fitted to the data.

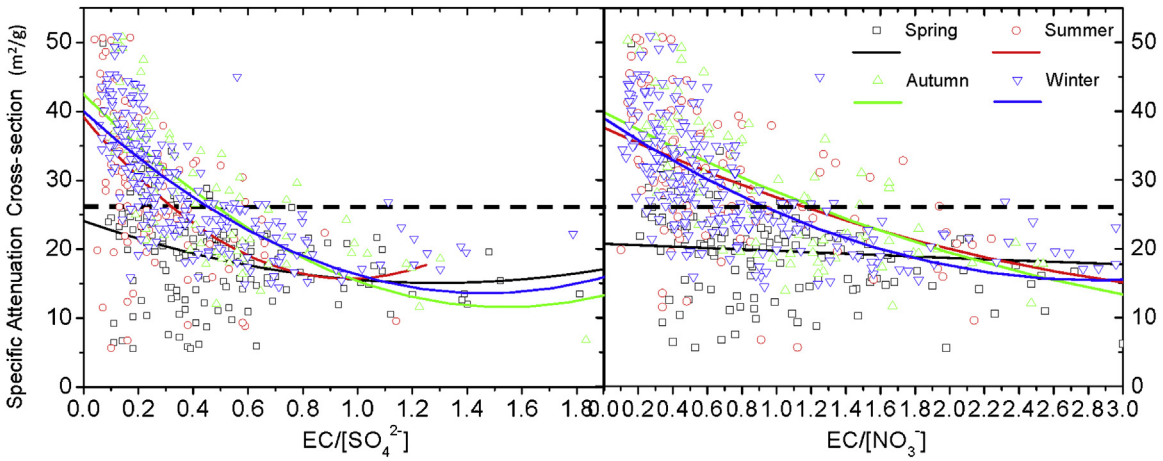

Fig. 6. Seasonal relationships between the σ_{ATN} and the EC/[SO_4^{2-}] and EC/[NO_3^-] ratios.

b_{abs} value for a pollution layer that originated from Mainland China during the ACE-Asia experiment was $21 \pm 8\,Mm^{-1}$. Mayol-Bracero et al. (2002) found the average b_{abs} value for a pollution layer that originated from the Indian subcontinent was $20 \pm 10\,Mm^{-1}$ during the INDOEX study. The annual average b_{abs} value was $244\,Mm^{-1}$ in Xi'an, exceeding these values by more than tenfold and demonstrating the strong light-absorbing nature of the urban atmosphere in northern China.

The artifacts associated with the Aethalometer measurements may affect the results. The Aethalometer uses a σ_{ATN} of $16.6\,m^2/g$ at 880 nm. However, these data are only the instrument measurements on the filter material, not the absorption coefficients of the BC particle in the air (Bodhaine, 1995; Park, Hansen, & Cho, 2010; Virkkula et al., 2007). The previous results show that the Aethalometer may overestimate light absorption (Collaud Coen et al., 2010), partially contributing to the high absorption efficiencies for EC.

Variability of σ_{ATN} versus the ratios of EC to $PM_{2.5}$, sulfate, and nitrate

Fig. 5 shows the variability of σ_{ATN} as a function of the EC mass fraction in $PM_{2.5}$. The σ_{ATN} values exhibited an exponential decrease when the EC mass fraction of $PM_{2.5}$ increased. Previous studies (Fuller, Malm, & Kreidenweis, 1999; Petzold et al., 1997) have shown that the light absorption efficiency of an internally mixed particle can be significantly enhanced when the EC mass fraction in the particle decreases. In this context, the results of our field experiments agree with the theoretical predictions. A simple model has been presented to describe the effects of light scattering particles on the specific attenuation cross-section (Petzold et al., 1997). According to this model, σ_{ATN} varies with the BC fraction of the total mass, f, as follows:

$$\sigma_{ATN}(f) = \sigma_{abs} + \left(\frac{1-f}{f}\right)\sigma_{scat}, \quad (3)$$

where f is the mass fraction of light absorbing matter, specifically $f = S_{abs}/(S_{abs} + S_{scat})$; S_{abs} and S_{scat} are the specific mass loadings of light absorbing and lightscattering particulate matter.

Eq. (3) relies on the following assumptions: BC is only the light absorbing material, and the non-graphitic fraction of the dry particulates is only the light scattering material. Several qualifiers are apparent for the relationship shown in Eq. (3): (a) light scattering enhances the specific attenuation cross-section without affecting the optical properties of the absorbing particles themselves, and (b) the light attenuation and absorption converge when increasing the mass fraction of the light absorbing components. When substituting $\sigma_{abs} = 4\,m^2/g$ in Eq. (3), the average values calculated for σ_{scat} were 1.0, 1.2, 1.5, and $1.2\,m^2/g$ in spring, summer, autumn, and winter, respectively in Xi'an. These results agree with the σ_{scat} of $1.2–2.5\,m^2/g$ found for urban sites in Germany (Petzold et al., 1997).

Fig. 6 shows that high average values for σ_{ATN} (34.3 and $41\,m^2/g$) were observed when the ratios of EC/[SO_4^{2-}] and EC/[NO_3^-] ratios were respectively below 0.2. For high ratios of EC/[SO_4^{2-}] (>1) and EC/[NO_3^-] (>1.4), σ_{ATN} was low and relatively stable with values of 17.8 and $22\,m^2/g$, respectively. Furthermore, σ_{ATN} exhibited an exponential decrease with increased ratios of EC/[SO_4^{2-}] and EC/[NO_3^-] during the summer, autumn and winter. The high levels of SO_4^{2-} (~35.6 μg/m³) and NO_3^- (~16.4 μg/m³) at Xi'an (Zhang et al., 2011) led to the low EC/[SO_4^{2-}] and EC/[NO_3^-] ratios. Particularly during winter, σ_{ATN} was affected by the large quantities of SO_4^{2-}, and NO_3^- that resulted from the coal burning necessary for domestic heating and other purposes. As noted above, the formation of secondary sulfate-rich particles also occurs during the summer at Xi'an due to the strong solar radiation, as well as the high temperatures, and RHs. The high values for σ_{ATN} obtained under these conditions can be explained by the dominance of the internal mixtures; these mixtures can contribute to a relatively stronger positive forcing from the EC.

A further examination of the variations in σ_{ATN} showed that the σ_{ATN} converged asymptotically when the ambient EC concentrations increased and diverged because the EC/$PM_{2.5}$, EC/[SO_4^{2-}] and EC/[NO_3^-] ratios were low. In summary, the high values for σ_{ATN} can be explained by the internal mixtures that are favored when sulfate and nitrate are abundant. In contrast, the low values for σ_{ATN} are consistent with the predominance of externally mixed EC particles.

Conclusions

A two-year study was conducted in Xi'an to characterize the carbonaceous composition of urban aerosols and to understand the causes for the variations in the light attenuation characteristics of the particles. σ_{ATN} exhibited a considerable seasonal variability, averaging 18.6, 24.2, 16.4, and $26.0\,m^2/g$ during the spring, summer, autumn, and winter, respectively, and an overall annual average of $23.0\,m^2/g$. These variations were mainly attributed to changes in the EC loadings and the formation of and mixing with secondary sulfate-/nitrate-rich particles. The relationships

involving σ_{ATN}, EC, EC/[SO_4^{2-}], and EC/[NO_3^-] led to temporal variations in the optical properties of the aerosols; specifically, the high values for σ_{ATN} were explained by the internal mixing of EC with sulfate and nitrate, while the low values for σ_{ATN} were consistent with the externally mixed EC particles. Additional studies should be undertaken to investigate whether these relationships are consistent across other urban areas in northern China.

Acknowledgements

This study was supported by the projects from the National Natural Science Foundation of China (41230641), the Ministry of Science & Technology (2012BAH31B03, 201209007), and the Shaanxi Government (2012KTZB03-01-01, 2011KTCQ03-04).

References

Andrea, M. O., & Gelencsér, A. (2006). Black carbon or brown carbon? The nature of light-absorbing carbonaceous aerosols. *Atmospheric Chemistry and Physics*, *6*, 3131–3148.

Arnott, W. P., Hamasha, K., Moosmüller, H., Sheridan, P., & Ogren, J. A. (2005). Towards aerosol light-absorption measurements with a 7-wavelength Aethalometer: Evaluation with a photoacoustic instrument and 3-wavelength nephelometer. *Aerosol Science and Technology*, *39*, 17–29.

Bergstrom, R. W. (1982). The optical properties of particulate elemental carbon. In G. T. Wolff, & R. L. Klimisch (Eds.), *Particulate carbon: Atmospheric life cycle* (pp. 43–49). New York: Plenum Press.

Bodhaine, B. A. (1995). Aerosol absorption measurements at Barrow, Mauna Loa and the south pole. *Journal of Geophysical Research: Atmospheres*, *100*(D5), 8967–8975.

Bohren, C. F., & Huffman, D. R. (1983). Absorption and scattering by a sphere. In *Absorption and scattering of light by small particles*. New York: Wiley-VCH Verlag GmbH & Co. KGaA.

Cao, J. J., Lee, S. C., Ho, K. F., Zhang, X. Y., Zou, S. C., Fung, K., et al. (2003). Characteristics of carbonaceous aerosol in Pearl River Delta Region, China during 2001 winter period. *Atmospheric Environment*, *37*, 1451–1460.

Cao, J. J., Wu, F., Chow, J. C., Lee, S. C., Li, Y., Chen, S. W., et al. (2005). Characterization and source apportionment of atmospheric organic and elemental carbon during fall and winter of 2003 in Xi'an, China. *Atmospheric Chemistry and Physics*, *5*, 3127–3137.

Cao, J. J., Lee, S. C., Zhang, X. Y., Chow, J. C., An, Z. S., Ho, K. F., et al. (2005). Characterization of airborne carbonate over a site on Asian Dust source regions during 2002 spring and its climatic and environmental significance. *Journal of Geophysical Research*, *110*, D03203. http://dx.doi.org/10.1029/2004JD005244

Cao, J. J., Lee, S. C., Chow, J. C., Watson, J. G., Ho, K. F., Zhang, R. J., et al. (2007). Spatial and seasonal distributions of carbonaceous aerosols over China. *Journal of Geophysical Research*, *112*, D22S11. http://dx.doi.org/10.1029/2006JD008205

Cao, J. J., Zhu, C. S., Chow, J. C., Watson, J. G., Han, Y. M., Wang, G. H., et al. (2009). Black carbon relationships with emissions and meteorology in Xi'an, China. *Atmospheric Research*, *94*, 194–202.

Cao, J. J., Shen, Z. X., Chow, J. C., Lee, S. C., Tie, X. X., Watson, J., et al. (2012). Chemical composition of $PM_{2.5}$ in the 14 Chinese cities. *Journal of the Air & Waste Management Association*, *62*, 1214–1226.

Chou, C. C. K., Chen, W. N., Chang, S. Y., Chen, T. K., & Huang, S. H. (2005). Specific absorption cross-section and elemental carbon content of urban aerosols. *Geophysical Research Letters*, *32*, L21808. http://dx.doi.org/10.1029/2005GL024301

Chow, J. C., & Watson, J. G. (2002). $PM_{2.5}$ carbonate concentrations at regionally representative interagency monitoring of protected visual environment sites. *Journal of Geophysical Research*, *107*(D21) http://dx.doi.org/10.1029/2001JD.000574. ICC6-1–ICC6-9

Clarke, A. D., & Charlson, R. J. (1985). Radiative properties of the background aerosol: Absorption component of extinction. *Science*, *229*, 263–265.

Collaud Coen, M., Weingartner, E., Apituley, A., Ceburnis, D., Fierz-Schmidhauser, R., Flentje, H., et al. (2010). Minimizing light absorption measurement artifacts of the Aethalometer: Evaluation of five correction algorithms. *Atmospheric Measurement Techniques*, *3*, 457–474.

Cooke, W. F., Liousse, C., Cachier, H., & Feichter, J. (1999). Construction of a 1×1 fossil fuel data set for carbonaceous aerosol and implementation and radiative impact in the ECHAM4 model. *Journal of Geophysical Research*, *104*, 22137–22162.

Crutzen, P. J., & Andreae, M. O. (1990). Biomass burning in the tropics: Impact on atmospheric chemical and biogeochemical cycles. *Science*, *250*, 1669–1678.

Fuller, K. A., Malm, W. C., & Kreidenweis, S. M. (1999). Effects of mixing on extinction by carbonaceous particles. *Journal of Geophysical Research*, *104*(D13), 15941–15954.

Hansen, A. D. A., Kapustin, V. N., Kopeikin, V. M., Gillette, D. A., & Bodhaine, B. A. (1993). Optical absorption by aerosol black carbon and dust in a desert region of central Asia. *Atmospheric Environment*, *27A*, 2527–2531.

Haywood, J. M., Roberts, D. L., Slingo, A., Edwards, J. M., & Shine, K. P. (1997). General circulation model calculations of the direct radiative forcing by anthropogenic sulfate and fossil-fuel soot aerosol. *Journal of Climate*, *10*, 1562–1577.

Jacobson, M. Z. (2000). A physically based treatment of elemental carbon optics: Implications for global direct forcing of aerosols. *Geophysical Research Letters*, *27*, 217–220.

Jacobson, M. Z. (2001). Strong radiative heating due to the mixing state of black carbon in atmospheric aerosols. *Nature*, *409*, 695–697.

Jeong, C. H., Hopke, P. K., Kim, E., & Lee, D. W. (2004). The comparison between thermal–optical transmittance elemental carbon and Aethalometer black carbon measured at multiple monitoring sites. *Atmospheric Environment*, *38*, 5193–5204.

Lavanchy, V. M. H., Gaggeler, H. W., Nyeki, S., & Baltensperger, U. (1999). Elemental carbon (EC) and black carbon (BC) measurements with a thermal method and an aethalometer at the high-alpine research station Jungfraujoch. *Atmospheric Environment*, *33*, 2759–2769.

Li, Y., Zhang, X. Y., Gong, S. L., Che, H. Z., Wang, D., Qu, W. J., & Su, J. Y. (2006). Comparison of EC and BC and evaluation of dust aerosol contribution to light absorption in Xi'an, China. *Environmental Monitoring and Assessment*, *120*, 301–312.

Liousse, C., Cachier, H., & Jennings, S. G. (1993). Optical and thermal measurements of black carbon aerosol content in different environments: Variation of the specific attenuation cross-section, sigma. *Atmospheric Environment*, *27*, 1203–1211.

Mader, B. T., Flagan, R. C., & Seinfeld, J. H. (2002). Airborne measurements of atmospheric carbonaceous aerosols during ACE-Asia. *Journal of Geophysical Research*, *107*(D23), 4704. http://dx.doi.org/10.1029/2002JD002221

Martins, J. V., Artaxo, P., Liousse, C., Reid, J. S., Hobbs, P. V., & Kaufman, Y. J. (1998). Effects of black carbon content, particle size, and mixing on light absorption by aerosols from biomass burning in Brazil. *Journal of Geophysical Research*, *103*(D24), 32041–32050.

Mayol-Bracero, O. L., Gabriel, R., Andreae, M. O., Kirchstetter, T. W., Novakov, T., Ogren, J., et al. (2002). Carbonaceous aerosols over the Indian Ocean during the Indian Ocean Experiment (INDOEX): Chemical characterization, optical properties, and probable sources. *Journal of Geophysical Research*, *107*(D19), 8030. http://dx.doi.org/10.1029/2000JD000039

Menon, S., Hansen, J., Nazarenko, L., & Luo, Y. F. (2002). Climate effects of black carbon aerosols in China and India. *Science*, *297*, 2250–2253.

Myhre, G., Stordal, F., Restad, K., & Isaksen, I. S. A. (1998). Estimation of the direct radiative forcing due to sulfate and soot aerosols. *Tellus B*, *50*, 463–477.

Novakov, T., & Corrigan, C. E. (1995). Thermal characterization of biomass smoke particles. *Mikrochimica Acta*, *119*, 157–166.

Park, S. S., Hansen, A. D. A., & Cho, S. Y. (2010). Measurement of real time black carbon for investigating spot loading effects of Aethalometer data. *Atmospheric Environment*, *44*(11), 1449–1455.

Petzold, A., Kopp, C., & Niessner, R. (1997). The dependence of the specific attenuation cross-section on black carbon mass fraction and particle size. *Atmospheric Environment*, *31*, 661–672.

Ramanathan, V., Chung, C., Kim, D., Bettge, T., Buja, L., Kiehl, J. T., et al. (2005). Atmospheric brown clouds: Impacts on South Asian climate and hydrological cycle. *Proceedings of the National Academy of Sciences of the United States of America*, *102*, 5326–5333.

Rosen, H., & Hansen, A. D. A. (1984). Role of combustion-generated carbon particles in the absorption of solar radiation in the Arctic Haze. *Geophysical Research Letters*, *11*, 461–464.

Virkkula, A., Mäkelä, T., Hillamo, R., Yli-Tuomi, T., Hirsikko, A., Hämeri, K., et al. (2007). A simple procedure for correcting loading effects of aethalometer data. *Journal of the Air & Waste Management Association*, *57*(10), 1214–1222.

Weingartner, E., Saathoff, H., Schnaiter, M., Streit, N., Bitnar, B., & Baltensperger, U. (2003). Absorption of light by soot particles: Determination of the absorption coefficient by means of Aethalometers. *Journal of Aerosol Science*, *34*, 1445–1463.

Zhang, X. Y., Gong, S. L., Arimoto, R., Shen, Z. X., Mei, F. M., Wang, D., et al. (2003). Characterization and temporal variation of Asian dust aerosol from a site in the northern Chinese deserts. *Journal of Atmospheric Chemistry*, *44*, 241–257.

Zhang, X. Y., Wang, Y. Q., Zhang, X. C., Guo, W., Niu, T., Gong, S. L., et al. (2008). Aerosol monitoring at multiple locations in China: Contributions of EC and dust to aerosol light absorption. *Tellus B*, *60*(4), 647–656.

Zhang, T., Cao, J. J., Tie, X. X., Shen, Z. X., Liu, S. X., Ding, H., et al. (2011). Water-soluble ions in atmospheric aerosols measured in Xi'an, China: Seasonal variations and sources. *Atmospheric Research*, *102*(1), 110–119.